ELSEVIER

Journal of Nuclear Materials 282 (2000) 75–82

journal of nuclear materials

www.elsevier.nl/locate/jnucmat

Dissolution of UO_2 in Boom clay water in oxidizing conditions: an XPS study

S. Guilbert [a,*], M.J. Guittet [b], N. Barré [a], M. Gautier-Soyer [b], P. Trocellier [a], D. Gosset [c], Z. Andriambololona [d]

[a] *DSM/DRECAM/LPS, CEA Saclay, Bât 637, 91191 Gif sur Yvette cedex, France*
[b] *DSM/DRECAM/SRSIM, CEA Saclay, Bât 462, 91191 Gif sur Yvette cedex, France*
[c] *DRN/DMT/LEMA, CEA Saclay, Bât 522, 91191 Gif sur Yvette cedex, France*
[d] *ANDRA, Parc de la Croix Blanche, 1-7 Rue Jean Monnet, 92298 Châtenay Malabry cedex, France*

Received 6 December 1999; accepted 30 May 2000

Abstract

The solubility behavior of uranium dioxide was studied under oxidizing conditions in the Belgian Boom clay water at 25°C up to 323 days. X-ray photoelectron spectroscopy analyses reveal that both U(VI) and U(IV) oxidation states are present in the altered layer. The U(VI)/U(IV) ratio in this altered layer increases up to 43 days and then remains constant throughout the whole test. In the leachate the uranium concentration also increases up to 43 days and then stabilizes. It is rather unlikely that the altered layer formed on the surface controls thermodynamically the uranium solubility. It is rather probable that the system has reached a pseudo-equilibrium governed by kinetics.

PACS: 82.65.i; 81.65.Mq; 81.05.Je

1. Introduction

The chemical stability of a nuclear waste repository is defined by its resistance to radionuclide release to the biosphere. This stability is dependent on the chemical stability of the spent fuel matrix itself, that is to say UO_2. Under oxidizing conditions, UO_2 is thermodynamically unstable. Therefore, an oxidation process occurs on its surface leading afterwards to dissolution. So if spent fuel should be disposed, a knowledge of the oxidation of UO_2 in contact with water would be needed to predict the release of radionuclides.

Under reducing conditions prevailing in a repository, UO_2 is the stable uranium solid. However, due to α-radiolysis, oxidizing conditions cannot be excluded. Under these conditions, UO_2 is not thermodynamically stable. The UO_2 surface undergoes oxidation to higher oxides, leading to subsequent dissolution and possible secondary phases formation, depending on the availability of oxygen and on the composition of the groundwater [1]. A large amount of data is available in the literature concerning the dissolution behavior of UO_2 in granitic groundwater [1–3], but fewer experiments have been performed in clay water.

XPS appears to be an appropriate technique to study the oxidation–dissolution process undergone by a UO_2 surface. As described by Allen et al. [4], the dry oxidation of UO_2 at 298 K leads to the progressive growth of a shake up satellite positioned at 8.2 eV of the high binding energy side of the U4f core levels. This satellite is characteristic of the UO_{2+x} surface. McIntyre [5] has followed the stoichiometric changes of a UO_2 electrode surface, by observing the chemical shift of $U4f^{7/2}$ photoelectron peak vs applied bias.

In this paper, we present the results of dissolution experiments of unirradiated UO_2 pellets in Boom clay water under oxidizing conditions. Our approach is based on the coupling of leachate analyses and the UO_2

* Corresponding author.

0022-3115/00/$ - see front matter
PII: S0022-3115(00)00239-7

surface characterization by XPS. The purpose of this study is to determine the evolution of the U(VI)/U(IV) ratio as oxidation–dissolution proceeds and to identify the nature of the solubility limiting phase in oxidizing conditions.

2. Experimental

2.1. Corrosion experiments

The experiments involve exposure of sintered ^{235}U depleted pellets of uranium dioxide to synthetic clay water. They were carried out under constant CO_2 (0.01 atm) and O_2 (0.2 atm) bubbling. The composition and pH of the synthetic oxidized Boom clay water are given in Table 1. The pellets were 8 mm in diameter and 2 mm thick. Their surfaces were polished on both sides using 20 μm Al_2O_3 powder. They were leached up to 323 days in oxidizing conditions (geometrical surface to volume ratio 1.5 cm^{-1}). Both leachates and oxidized surfaces were characterized.

2.2. Analytical methods

The uranium concentration in the leachates was measured by Inductively Coupled Plasma Mass Spectrometry (VG Plasmaquad PQ-2+) in filtered (0.45 μm) aliquots. The contents of anions and cations in the solutions were analyzed by Ion Chromatography (DIONEX DX-120). The pH and Eh were measured under constant O_2 (0.2 atm) and CO_2 (0.01 atm) bubbling.

The presence of secondary uranium phases on the surface of the pellets was checked by scanning electron microscopy (SEM) (Cambridge Stereoscan 120) coupled with X-ray microanalysis.

The altered layer on the surface of the pellets was characterized by X-ray Photoelectron Spectroscopy (XPS). For each leaching test, two samples were characterized by XPS and one was characterized after ion etching of the oxidized layer. Besides leached UO_2, we have also studied clean UO_2, unleached UO_2, U_3O_8 and UO_3 as references. Commercial U_3O_8 and UO_3 powders supplied by Prolabo were dried at 400°C for 24 and 48 h, respectively. The absence of OH and H_2O was checked by Infra Red Spectroscopy (FTIR Model Nicolet 550) for both powders. A synthesis of crystalline UO_3 by heating $UO_2(NO_3)_2$, $6H_2O$ (Prolabo) 25 h at 500°C was also performed. The powders were pressed onto indium foil before analysis. Clean UO_2 was produced by ion etching of the oxidized surface on the UO_2 pellet with an Ar beam (2 kV, 1 min, 12 μA). Unleached UO_2, U_3O_8 and UO_3 were also characterized by X-ray Diffraction (XRD). XRD measurements were performed on a curved detector INEL CPS 120 using the $CuK\alpha_1$ line ($\lambda = 1.540598$ Å) and calibrated in position with a Y_2O_3 standard ($a = 10.6033$ Å) and in intensity with a ^{65}Zn sample emitting 8 keV X-rays; the spectra were recorded in the 2θ 20–140° range in 4096 channels 0.029° wide. The XRD patterns for UO_2 and U_3O_8 match JCPDS card number 76–1118 for UO_2 (cubic) and number 74–2101 for U_3O_8 (orthorhombic). The commercial UO_3 powder is amorphous. The synthesized UO_3 matches the JCPDS card number 71–0190 (tetragonal) (Fig. 1).

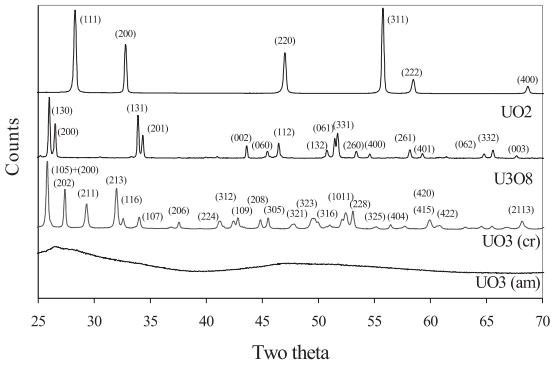

Fig. 1. X-ray diffraction patterns of UO_2, U_3O_8 and UO_3.

2.3. XPS apparatus

The spectrometer used in this work was a VG Scientific Escalab Mark II. X-ray photoelectron spectra were produced using monochromatic Al Kα radiation (1486.6 eV). The full width at half maximum of the silver $3d^{5/2}$ is 0.7 eV. Low-resolution survey spectra were recorded for the 0–1250 eV region to determine the elements present in the sample and to check for surface contamination. High-resolution spectra were recorded for the U4f (374–404 eV), O1s (525–540 eV), C1s (280–292 eV) and valence band (−3–37 eV) regions to determine the chemical state of these elements. Calibration was achieved by referring to the C1s binding energy of contamination carbon at 284.6 eV.

Table 1
Composition of the oxidized Boom clay water

Species	Na^+	Ca^{2+}	Cl^-	Mg^{2+}	K^+	Si_{aq}	SO_4^{2-}	HCO_3^-	pH	I (mol/l)
mmol/l	83.5	2.7	0.36	4.7	1.9	0.07	47.6	6.5	7.5	0.16
ppm	1920	108	12.8	114	74	2	4570	396		

3. Results

3.1. Leachates

In the leachate, the uranium concentration increases up to 43 days and then remains constant at 140 μmol/l. The results are plotted as uranium content in filtered aliquots versus leaching time in Fig. 2. The anions and cations contents of the leachate are not modified by leaching.

3.2. Solid samples

3.2.1. SEM

The morphology of the uranium dioxide observed by SEM changes as leaching goes on (Fig. 3(a) and (b)). In places we observed that the grains were larger after leaching. The analysis by energy dispersive X-ray spectrometry (EDS) of these spots showed no other element than uranium and oxygen.

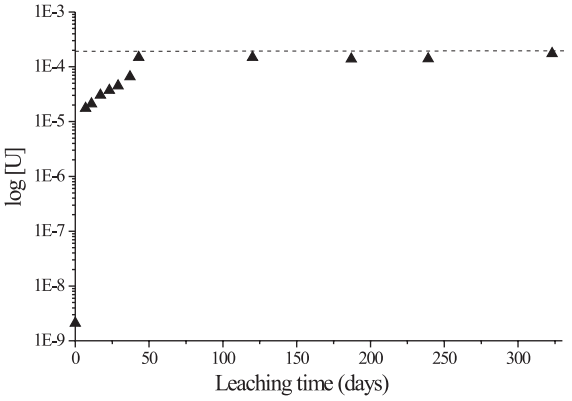

Fig. 2. Uranium concentration versus time in the filtered aliquots.

3.2.2. XPS

3.2.2.1. Clean UO_2, U_3O_8 and UO_3. Fig. 4 shows the spectra for the U4f, O1s and valence regions of clean UO_2, U_3O_8 and amorphous UO_3. Binding energy and line width for the $U4f^{7/2}$ and O1s peaks are presented in Table 2, included for comparison are those values reported by Allen [4]. Agreement between the two sets of data is good, except for the full widths at half maximum since Allen used a non-monochromatic Al Kα radiation.

Uranium trioxide is an insulator. Nevertheless, no charging effect was observed when recording the spectra of the amorphous UO_3. On the other hand, spectra of the crystalline UO_3 were recorded with the aid of a 'flood gun', in order to neutralize the charging effect, but in spite of it, the spectra were distorted. The spectra were also recorded after evaporating a thin film of gold onto the surface sample (1 nm), without conclusive results.

The energy separation from the fundamental lines to the satellites characterizes the chemical bond and it differs from one oxide to the other. Pireaux observes satellites in γUO_3 spaced from the fundamental lines by about 3.7 and 10.6 eV, whereas in U_3O_8 they are spaced by 4.0, 8.0 and 10.0 eV [7]. The differences in the binding energies of the U4f and O1s core levels might be due to the methods used to reference binding energy.

The ion etched UO_2 spectrum shows two sharp U4f bands associated with two satellites with a separation of 6.85 eV (close to the value of 6.9 eV reported by Allen et al. [6]) from the main peak. These satellites are due to discrete energy loss by 'shake up' processes (excitation of an electron from the O2p-U bonding levels to partially occupied or unoccupied metal 5f levels) [4]. Those satellites are not present in the U_3O_8 spectra. Besides, a

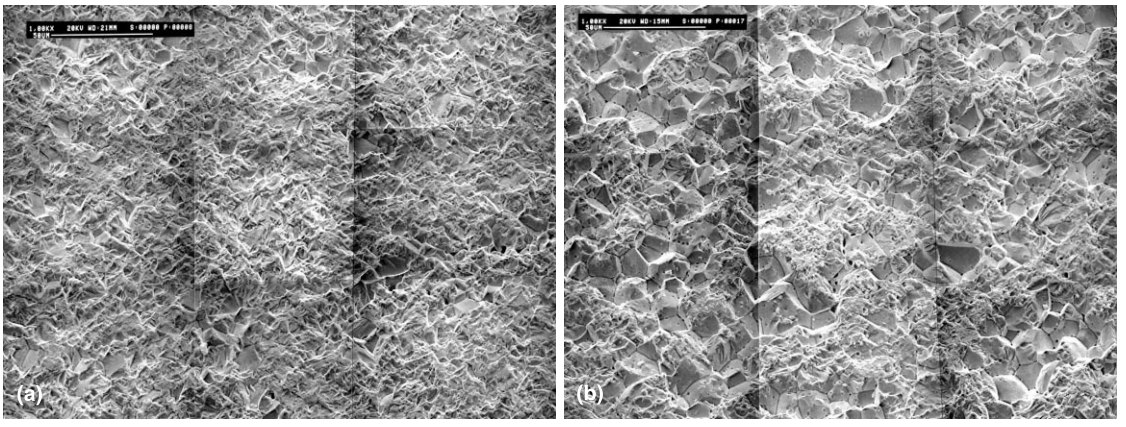

Fig. 3. (a) SEM micrograph of the surface of the unaltered sample, (b) SEM micrograph of the surface of the 323-day leached UO_2 in Boom clay water in oxidizing conditions.

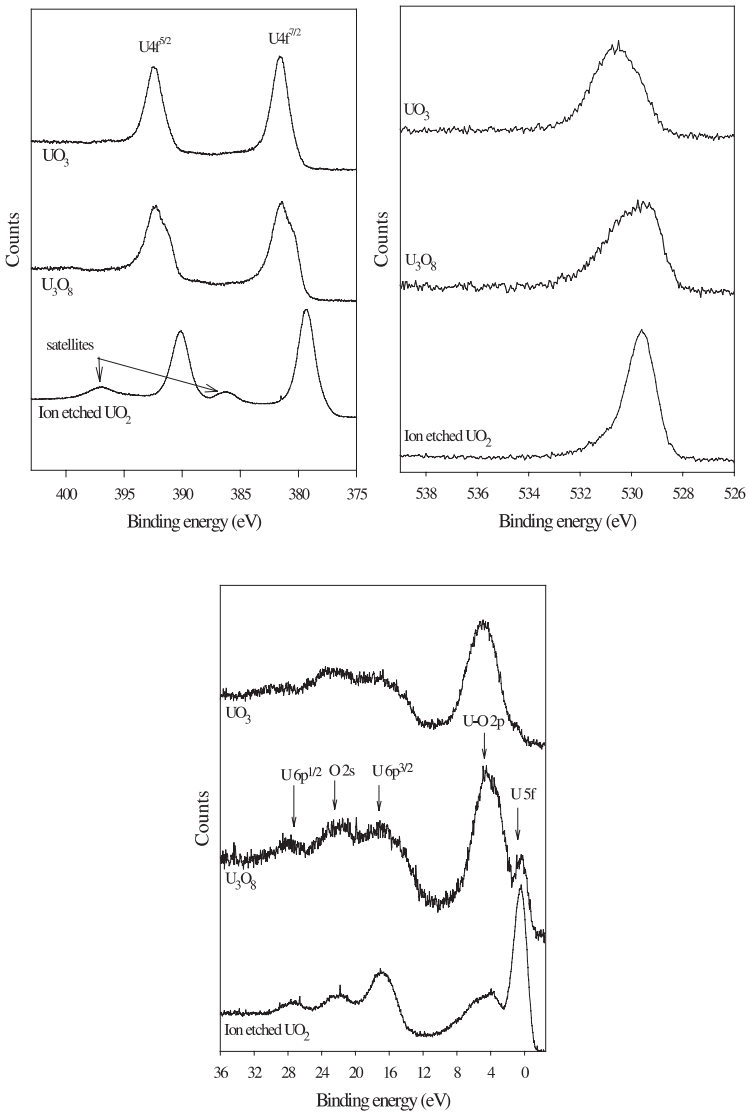

Fig. 4. U4f, O1s and valence region for clean UO_2, U_3O_8 and UO_3.

Table 2
Binding energies and full widths at half maximum of the $U4f^{7/2}$ and O1s core levels in clean UO_2, U_3O_8 and UO_3

Samples	Binding energy (eV)				
	$U4f^{7/2}$	fwhm	Satellites position	O1s	fwhm
Ion etched UO_2	379.35	1.7	6.85	529.6	1.3
UO_2	379.5 ± 0.05	1.7 ± 0.05	7.0 ± 0.05	529.8 ± 0.05	1.2 ± 0.05
U_3O_8	381.3	2.1		530.0	2.05
UO_3	381.6	1.7		530.6	2.0
UO_2 [4]	380.3	2.8	6.9	530.4	
U_3O_8 [4]	381.1	2.7	7.8	530.1	2.4
γUO_3 [4]	381.9	3.2		528.9	2.5

chemical shift to higher binding energy and a broadening of the U4f core levels are observed. This is due to the U(VI) component in U_3O_8. In the valence region, the intensity of the U5f line decreases as the O/U ratio increases and in the UO_3 spectra, this line can no longer be observed. The intensity of the O2p-U line also increases as the O/U ratio increases. This phenomenon is due to the electron transfer from the localized 5f states into the 'bonding' molecular orbitals which are predominately O2p in character as the oxidation increases [8]. The U_3O_8 and UO_3 samples have broader O1s band than UO_2, this is probably due to different oxygen environment.

3.2.2.2. Unleached, leached and leached+ion etched samples. Four unleached UO_2 samples were also characterized by XPS. By normalization of the surface of the $U4f^{7/2}$ and the O1s orbitals of those samples, we determined a mean O/U ratio of 2.1, indicating a slight surface oxidation of the unleached UO_2. Fig. 5 shows the spectra for the U4f, O1s and valence regions for the unleached, the 239-day leached and the 239-day leached + ion etched samples. Binding energy and line width for the $U4f^{7/2}$ and O1s peaks are presented in Table 3 as a function of leaching time.

A chemical shift up to 0.9–1.0 eV to higher binding energy and a slight broadening of the $U4f^{7/2}$ level occur

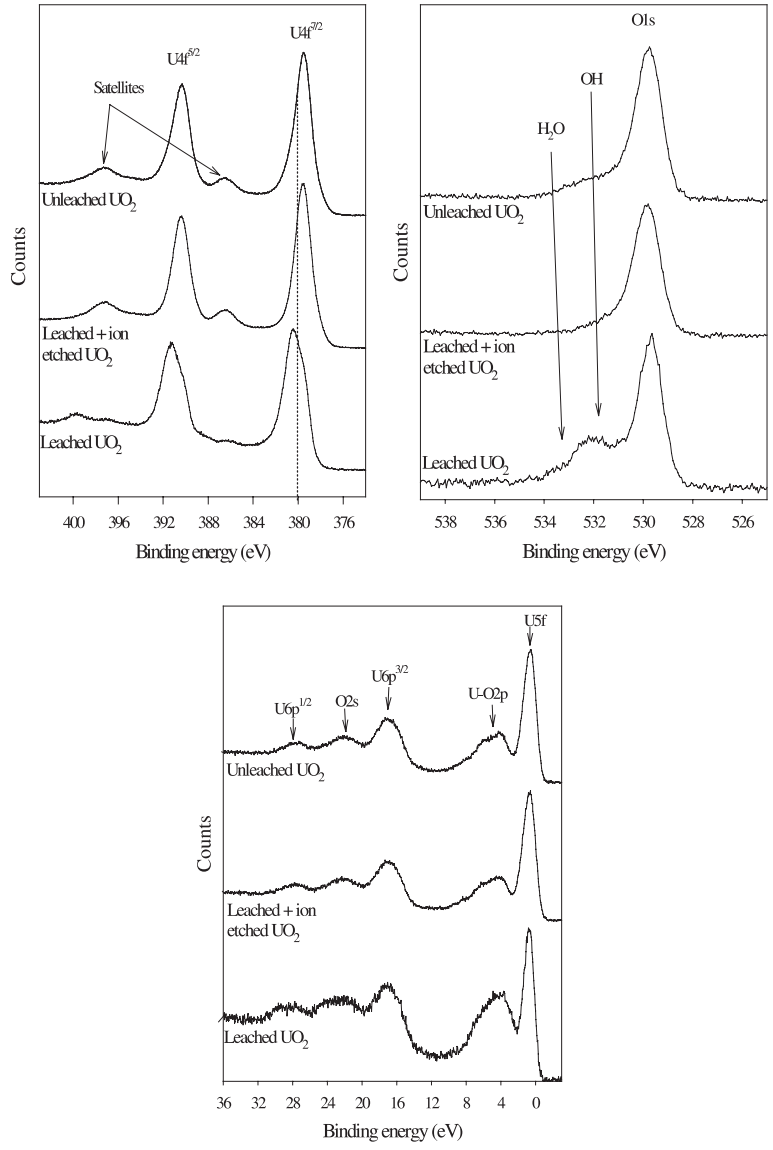

Fig. 5. U4f, O1s and valence region for unleached, 239-day leached and 239-day leached + ion etched UO_2.

Table 3
Binding energies and fwhm (in parentheses) of the $U4f^{7/2}$ and O1s core levels in unleached and leached UO_2 and U(VI)/U(IV) ratio

Samples	Binding energy (eV)					U(VI)/U(IV)
	$U4f^{7/2}$	Satellites position	$U4f^{5/2}$	Satellites position	O1s	
Unleached UO_2	379.5 ± 0.05 (1.7 ± 0.05)	7 ± 0.05	390.4 ± 0.05	6.8 ± 0.10	529.8 ± 0.05 (1.2 ± 0.05)	0.09 ± 0.02
7-day leached	379.7 (2.3)	6.35	390.5 (2.3)	6.4, 8.6	529.55 (1.3)	1.0
11-day leached	380.0 (2.3)	6.0	390.5 (2.3)	6.2, 8.6	529.45 (1.2)	0.95
17-day leached	380.2 (2.2)	5.9	391.1 (2.2)	5.7, 8.2	529.6 (1.0)	1.1
23-day leached	380.25 (2.2)	5.85	391.15 (2.3)	5.9, 8.5	529.8 (1.2)	1.2
29-day leached	380.25 (2.35)	5.6	391.5 (2.3)	5.45, 8.35	530.0 (1.3)	1.3
37-day leached	380.6 (2.3)	5.8	391.5 (2.3)	5.75, 8.35	530.0 (1.2)	1.25
43-day leached	380.4 (2.2)	5.6	391.25 (2.2)	5.65, 8.35	529.6 (1.1)	1.65
120-day leached	380.25 (2.3)	5.6	391.1 (2.3)	5.1, 8.3	529.55 (1.0)	1.45
187-day leached	380.3 (2.2)	5.65	391.1 (2.2)	5.6, 8.3	529.6 (1.1)	1.5
239-day leached	380.4 (2.3)	5.8	391.25 (2.3)	5.8, 8.35	529.65 (1.2)	1.5
323-day leached	380.35 (2.3)	5.65	391.15 (2.2)	5.5, 8.4	529.65 (1.1)	1.5

on exposing the UO_2 surface to clay water. The ~6.8–7.0 eV shake up satellites associated with the U4f bands disappear and new satellites at ~8.3 and 5.7 eV appear. A chemical shift of ~0.2 eV to the lower binding energy side and a broadening on the higher binding energy side of the O1s core level are also observed. Concurrent with these changes, the intensity of the U5f level compared to the O2p-U band decreases in the valence region. The broadening on the higher binding energy side of O1s indicates the presence of hydroxyl and water species in the sample surface. The chemical shift to higher binding energy and the broadening of the U4f core levels are due to the apparition of the U(VI) component in the $U4f^{7/2}$ peak. All these changes in binding energy, satellites position, peak profile and intensity are due to surface oxidation [6]. This oxidation takes place through the incorporation of oxygen at interstitial sites, and as a consequence an oxygen 'cluster' called Willis cluster is created. The new satellite at 8.3 eV could be assigned to a charge transfer of an electron from the oxygen cluster to metal 5f or 6d levels [4]. The U5f band intensity decrease is due to the electron transfer from the localized 5f states into the 'bonding' molecular orbitals as oxidation proceeds.

Those changes are no longer observed on the leached + ion etched samples. The leached + ion etched samples spectra are almost the same as the unleached ones (Table 4).

It is worth mentioning here that sodium and calcium were sometimes found at trace level on the surface of the pellets. These elements are probably only sorbed on the surface of the samples.

4. Discussion

The $U4f^{7/2}$ photoelectron line is very sensitive to the chemical state of the uranium atoms, and can be resolved into U(VI) and U(IV) components to determine their relative amounts at the sample surface [5]. We have determined the full width at half maximum (fwhm) of the U(VI) and U(IV) components from the UO_3 and the clean UO_2 reference samples (Table 2). The bands due to U(VI) and U(IV) are supposed to be 2.1 eV apart

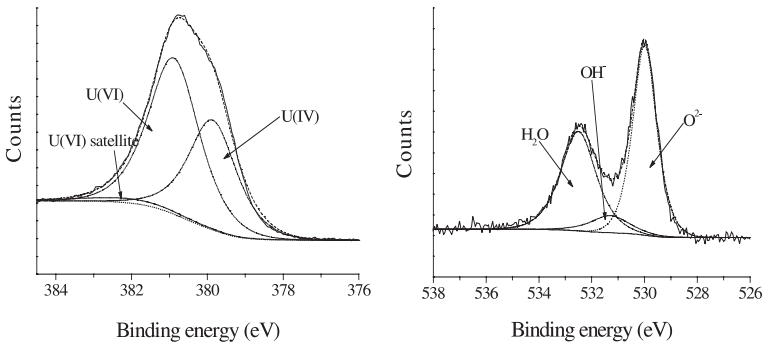

Fig. 6. Resolution of the $U4f^{7/2}$ and the O1s bands.

Table 4
Binding energies and fwhm (in parenthesis) of the $U4f^{7/2}$ and O1s core levels in leached and leached + ion etched UO_2 and U(VI)/U(IV) ratio

Samples		Binding energy (eV)	
		Leached	Leached ± ion etched
43-day leached	$U4f^{7/2}$	380.4 (2.2)	379.65 (1.8)
	Satellite	5.6	6.8
	O1s	529.6 (1.1)	529.9 (1.4)
	U(VI)/U(IV)	1.65	0.1
120-day leached	$U4f^{7/2}$	380.25 (2.3)	379.45 (1.7)
	Satellite	5.6	6.85
	O1s	529.55 (1.0)	529.7 (1.2)
	U(VI)/U(IV)	1.45	0.15
187-day leached	$U4f^{7/2}$	380.3 (2.2)	379.5 (1.7)
	Satellite	5.65	6.8
	O1s	529.6 (1.1)	529.65 (1.2)
	U(VI)/U(IV)	1.5	0.1
239-day leached	$U4f^{7/2}$	380.4 (2.3)	379.55 (1.7)
	Satellite	5.65	6.8
	O1s	529.65 (1.2)	529.85 (1.2)
	U(VI)/U(IV)	1.5	0
323-day leached	$U4f^{7/2}$	380.35 (2.3)	379.6 (1.7)
	Satellite	5.65	6.8
	O1s	529.65 (1.1)	529.95 (1.6)
	U(VI)/U(IV)	1.5	0.15

according to UO_2 and UO_3 reference samples. Nevertheless when resolving the $U4f^{7/2}$ peak of U_3O_8 we found the U(VI) and U(IV) components only 1.05 eV apart. It is not surprising since binding energy depends on both the valence state and the local structure around the studied atom. So when resolving the $U4f^{7/2}$ peak of the leached samples into U(VI) and U(IV) components, we tried to keep these parameters (U(VI) and U(IV) fwhm and the 1.05 eV difference between the two components) constant. The results are presented in Table 3 and in Fig. 6. The O1s peak was also resolved into metal-oxide (O^{2-}), hydroxyl (OH^-) and water (H_2O) components in the same way (Fig. 6) [9].

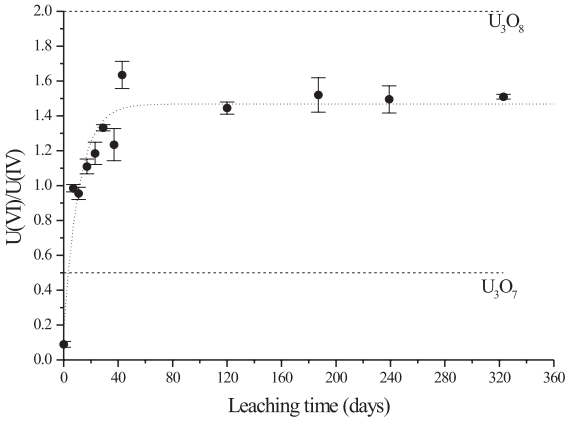

Fig. 7. Time evolution of the U(VI)/U(IV) ratio in the UO_2 surface exposed to clay water.

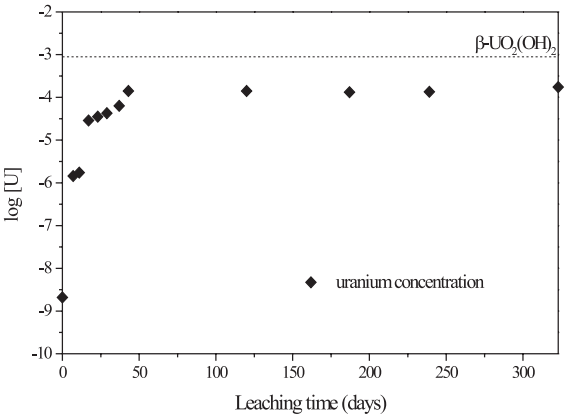

Fig. 8. Measured concentrations of uranium in filtered aliquots as a function of leaching time. The line represents the uranium solubility of schoepite (β-$UO_2(OH_2)$).

The U(VI)/U(IV) ratio of the unleached UO_2 is never higher than 0.1. In all samples exposed to clay water, this ratio is higher than in the unleached UO_2. The ratio is $\leqslant 2$ indicating that the surface has been oxidized to phases with average oxidation state lower than that in U_3O_8. This ratio increases with time up to 43 days and then remains constant around 1.5 ± 0.1 (Fig. 7). Similar observations have also been reported by Casas et al. [10]. The leached samples have also $(OH^-)/O^{2-}$ and $(H_2O)/O^{2-}$ ratios higher than that in unleached UO_2. After cleaning with the Ar beam, the U(VI)/U(IV) ratio is lower than that in unleached sample and the $(OH^-)/O^{2-}$ and $(H_2O)/O^{2-}$ ratios are the same as in the unleached UO_2. The results of the resolution of the O1s photoelectron line into metal-oxide (O^{2-}), hydroxyl (OH^-) and water (H_2O) components are not presented in Table 3 because no clear trend could be drawn.

Nevertheless these results indicate that the oxidized layer due to leaching has been removed by the ion etching. The oxidized film thickness should be less than 1 nm thickness removed by the Ar beam.

In the leachate, the uranium concentration also increases up to 43 days and then remains constant at 140 μmol/l (Fig. 2). The steady-state uranium concentration should be controlled by some kind of oxidized phase. The dissolution mechanism in oxidizing conditions involves the formation of an oxidized layer, subsequent dissolution of this layer and formation of UO_3 hydrate (schoepite) if sufficient oxygen is available [1]. We have determined the uranium concentration in equilibrium with schoepite with the geochemical code PHREEQC [11] using the thermodynamical data of Grenthe et al. [12]. The calculated solubility of schoepite is included in Fig. 8. It is in agreement with the experimental concentration, however, aside from the larger grains on the surface of the pellets, no uranium secondary phase was found by SEM. Moreover, it is unlikely that such a thin altered layer (<1 nm) would be able to control thermodynamically the uranium solubility. It is rather probable that the system has reached a pseudo-equilibrium governed by kinetics. Further experimental work should be devoted to enhance surface sensitivity in order to determine more accurately the composition of this altered layer, that is to say if it is a mixture of U(VI) and U(IV) or only U(VI) oxide.

5. Conclusion

The solubility behavior of uranium dioxide was studied under oxidizing conditions in the Belgian Boom clay water at 25°C up to 323 days. After 43 days a steady state between the solid and the leachate has been reached. It is likely that the system has reached a pseudo-equilibrium governed by kinetics. An 1 nm thick altered layer has formed on the surface of the pellets in which both U(VI) and U(IV) oxidation states are present and hydration–hydroxylation has occurred. The U(VI)/U(IV) ratio in this altered layer is around 1.5, smaller than the theoretical ratio in U_3O_8. Further experimental work is in progress in order to determine more accurately the composition of this altered layer.

Acknowledgements

This work is partially supported by a grant from the French Agency for Nuclear Waste Management (ANDRA) and from the French Atomic Energy Commission (CEA). S.G. is grateful to Pr Joan de Pablo of the Universitat Politècnica Catalunya and to Dr Jean Jacques Ehrhardt of the Laboratoire de Chimie Physique pour l'Environnement (CNRS) for helpful discussions. The authors wish to thank also the anonymous reviewers for useful comments.

References

[1] K. Ollila, Mater. Res. Soc. Symp. Proc. 465 (1997) 549.
[2] J. Bruno, I. Casas, A. Sandino, J. Nucl. Mater. 190 (1992) 61.
[3] I. Casas, J. Bruno, E. Cera, R.J. Finch, R.C. Ewing, SKB Technical Report 94-16, 1994.
[4] G.C. Allen, P.M. Tucker, J.W. Tyler, J. Phys. Chem. 86 (1982) 224.
[5] N.S. McIntyre, S. Sunder, D.W. Shoesmith, F.W. Stanchell, J. Vac. Sci. Technol. 18 (3) (1981) 714.
[6] G.C. Allen, J.A. Crofts, M.T. Curtis, P.M. Tucker, D. Chadwick, P.J. Hampson, J. Chem. Soc., Dalton Trans. (1974) 1296.
[7] J.J. Pireaux, J. Riga, E. Thibaut, C. Tenret-Noël, R. Caudano, J.J. Verbist, Chem. Phys. 22 (1977) 113.
[8] B.W. Veal, D.J. Lam, Phys. Lett. A 49 (1974) 466.
[9] E. McCafferty, J.P. Wightman, Surf. Interface Anal. 26 (1998) 549.
[10] I. Casas, J. Giménez, V. Martí, M.E. Torrero, J. de Pablo, Radio. Acta 66&67 (1994) 23.
[11] D.L. Parkhurst, US Geological Survey, Water Resources Investigations Report 95-4227, 1995.
[12] I. Grenthe, J. Fuger, R.J.M. Konings, R.J. Lemire, A.B. Muller, C. Nguyen-Trung, H. Wanner, in: H. Wanner, I. Forest (Eds.), Chemical Thermodynamics of Uranium, OECD Nuclear Energy Agency, 1992.